SCISPACE
formerly Typeset

Open access • Journal Article • DOI:10.2514/3.7736

Acoustic resonances and sound scattering by a shear layer — Source link

S. P. Koutsoyannis, K. Karamcheti, D. C. Galant

Institutions: Stanford University, Ames Research Center

Published on: 01 Dec 1980 - AIAA Journal (American Institute of Aeronautics and Astronautics (AIAA))

Topics: Reflection (physics), Reflection coefficient, Brewster's angle, Vortex sheet and Total internal reflection

Related papers:

- Characterization of acoustic disturbances in linearly sheared flows
- Effect of shear on duct wall impedance
- Propagation of Sound Waves through a Linear Shear Layer
- The Scattering of Sound by a Simple Shear Layer
- Problems in flow acoustics

Share this paper:

View more about this paper here: https://typeset.io/papers/acoustic-resonances-and-sound-scattering-by-a-shear-layer-39myj4t6iw

CR-166181
(D. Hickey)

JOINT INSTITUTE FOR AERONAUTICS AND ACOUSTICS

NASA
National Aeronautics and
Space Administration
Ames Research Center

Stanford University

JIAA TR - 20

ACOUSTIC RESONANCES AND SOUND SCATTERING BY A SHEAR LAYER

S.P. Koutsoyannis, K. Karamcheti, and D.C. Galant

JUN 1981
RECEIVED
NASA STI FACILITY
ACCESS DEPT.

STANFORD UNIVERSITY
Department of Aeronautics and Astronautics
Stanford, California 94305

RECEIVED
NASA STI FACILITY
ACCESS DEPT.

SEPTEMBER 1979

JIAA TR - 20

ACOUSTIC RESONANCES AND SOUND SCATTERING BY A SHEAR LAYER

S.P. KOUTSOYANNIS, K. KARAMCHETI,

AND D.C. GALANT

SEPTEMBER 1979

The work here presented has been supported by the National Aeronautics and Space Administration under NASA Grant 2233-6 and NASA 2308-1 to the Joint Institute for Aeronautics and Acoustics

TABLE OF CONTENTS

ABSTRACT 1

NOMENCLATURE 3

I. Introduction 5

II. The Expression for the Energy Reflection Coefficient. 6

III. Numerical Evaluation of the Energy Reflection Coefficient R^2 13

IV. Limiting Behavior of the Reflection Coefficient. 17

V. Resonances for the Finite Thickness Thin Shear Layer. 20

VI. Conclusions. 22

REFERENCES 25

APPENDIX A A-1

A.1 Representation of the Velocity Potentials in the Regions A-1

i. Velocity Potential ϕ_ℓ for the Lower Region $z \leq 0$. A-1

ii. Velocity Potential ϕ_u in the Upper Region $z \geq z_1$ A-2

A.2 Definition of the Energy Reflection Coefficient A-5

A.3 Acoustic Energy Conservation. A-6

APPENDIX B B-1

ACKNOWLEDGEMENTS

The authors would like to acknowledge, Mr. Ramji Digumarthi, for helping in the calculations of the graphs and Miss Jill Izzarelli for her expert typing of the manuscript.

ACOUSTIC RESONANCES AND SOUND SCATTERING BY A SHEAR LAYER

S. P. Koutsoyannis and K. Karamcheti
Joint Institute for Aeronautics and Acoustics
Department of Aeronautics and Astronautics
Stanford University, Stanford, California 94305

and

D. C. Galant
National Aeronautics and Space Administration
Ames Research Center
Moffett Field, California 94035

ABSTRACT

We examine the reflection and transmission of plane waves by a finite thickness shear layer having a linear velocity profile and bounded by two otherwise uniform parallel flows. The pressure perturbation equation in the shear layer has been shown previously to have exact solutions in terms of Whittaker M-functions. It is shown that in addition to the angle of plane wave incidence and the relative Mach number of the flows bounding the shear layer, the scattering properties of the shear layer depend crucially on a parameter τ in such a manner that the case $\tau \to 0$ characterizes the long wavelength properties of the layer (with $\tau = 0$ being the vortex sheet) and the case $\tau \to \infty$ characterizes the short wavelength properties of the layer (Geometrical Acoustics). We have evaluated numerically the relevant Whittaker M-functions and using these values we have studied the behavior of the energy reflection coefficient for a number of cases (angle of incidence, Mach number and various values of the parameter τ) at which the corresponding vortex sheet is known to exhibit resonances (reflection coefficient $\to \infty$) and/or Brewster

angles (reflection coefficient → 0). We find that, unlike the vortex sheet, the finite thickness shear layer has no resonances or Brewster angles. Moreover we find that in general for $\tau \gtrsim 0.5$ the amplified reflection regime degenerates into the total reflection regime of geometrical acoustics even in the cases in which the corresponding vortex sheet has resonances. In contrast for the region of ordinary reflection we find that in the cases in which the corresponding vortex sheet does not have a Brewster angle the values of the reflection coefficient up to $\tau = 1$ follow quite closely those of the vortex sheet whereas for the cases for which the corresponding vortex sheet has a Brewster angle the magnitude of the reflection coefficient may be quite sensitive even to small changes of τ in certain cases, contrary to some previous results of Graham and Graham[1]. The results of the present studies indicate that caution should be exercised in uncritically modeling a finite thickness shear layer by a corresponding vortex sheet, a practice usually followed currently in noise research and aeroacoustics.

NOMENCLATURE

a	=	(constant) sound speed
a_{ij}	=	constant coefficients defined by eq. (12)
b	=	linear velocity profile slope [units: $(\text{time})^{-1}$]
f, g	=	the two independent solutions (eq. (9)) of eq. (7)
i	=	$\sqrt{-1}$
$\vec{k}$	=	wave vector of incident plane
k_x	=	x-component of wave vector $\vec{k}$
m	=	$\frac{3}{4}$; second index of the Whittaker M-functions.
p'	=	pressure perturbation
$p^{(1)}$, $p^{(2)}$	=	linear combinations of f and g.
$\vec{r}$	=	position vector
sgn	=	"sign of"
t	=	time
w	=	z-component of velocity perturbation
x, z	=	coordinates
A, B, C, D	=	expressions defined by eq. (14)
H	=	heaviside function
$M(z)$	=	local Mach number
M_1	=	upper fluid Mach number
M-functions	=	Whittaker M-functions
R^2	=	Energy reflection coefficient
$\bar{R} = R_1 \pm iR_2$	=	Complex reflection coefficient for the perturbation velocity potential.
$\bar{T} = T_1 \pm iT_2$	=	complex transmission coefficient for the perturbation velocity potential.
R.P.	=	"Real Part of"
$U(z)$	=	local mean speed

η = non-dimensional variable defined by eq. (5)

θ = incident wave angle (see Fig. (1))

κ = $\sin\theta$

τ = non-dimensional parameter defined by eq. (8)

ω = angular frequency of incident plane wave

ϕ_ℓ, ϕ_u = perturbation velocity potentials for the lower and upper regions respectively.

I. Introduction

The shear layer with a linear velocity profile has been the object of a number of studies. Küchemann[2] considered the stability of the boundary layer with a linear velocity profile. Pridmore-Brown[3] studied rectangular duct modes in a duct with the basic flow having a linear velocity profile. Graham and Graham[1] studied plane wave propagation through a linear veloicty profile shear layer. Goldstein and Rice[4] found an exact solution to the pressure perturbation equation in terms of linear combinations of parabolic cylinder functions of different order. We have reported earlier (see Koutsoyannis[5]) some preliminary results on sound propagation through a shear layer with a linear velocity profile using essentially Whittaker M-functions as the basic solutions of the pressure perturbation equation. Jones[6] studied the stability of such a layer for subsonic basic flow using our previous solution in terms of Whittaker M-functions. Recently Scott[7] examined wave propagation through a linear shear layer using the Goldstein and Rice[4] unwieldy solution. With the exception of Goldstein and Rice[4], Koutsoyannis[5], Jones[6] and Scott[7] the other investigators were concerned with either series or asymptotic solutions of the pressure perturbation equation in the shear layer region.

In the present study we are concerned with the behavior of the energy reflection coefficient for plane waves incident on a finite thickness shear alyer with a linear velocity profile and bounded by two uniform parallel flows. For that purpose we have evaluated numerically the solutions of the pressure perturbation equation in

terms of Whittaker M-functions and with the aid of these we have numerically evaluated the reflection coefficient for a number of typical cases involving the relevant parameters, i.e., the angle of incidence of the plane waves, the upper fluid Mach number and a characteristic parameter τ which represents a non-dimensional measure of the disturbance Strouhal number with respect to the disturbance Mach number in the mean flow direction (see Section IV.).

In section II below we shall derive the expression for the reflection coefficient in terms of the two basic solutions of the pressure perturbation equation (i.e., the Whittaker M-function solutions). In section III we shall summarize and discuss our numerical results on the variation of the reflection coefficient. In section IV we shall discuss various limiting cases including the vortex sheet and geometrical acoustics limits and in section V we shall give an analytical proof for the absence of resonances for a thin shear layer. The results of the present studies are then summarized in the final section VI. At the end, in Appendix A we discuss the representations of the perturbations in the three flow regions (see Figure 1), and the definition of the energy reflection coefficient as well as energy conservation and finally in Appendix B we give the general outline of the numerical scheme used to evaluate the Whittaker M-functions.

II. The Expression for the Energy Reflection Coefficient

Without loss of generality we may assume that the layer with the linear velocity profile is bounded by two uniform flows, one of which is at relative rest, as shown in Figure 1, i.e., we assume the

following two-dimensional [in the (x,z) plane] inviscid compressible shear layer characterized by the mean continuous velocity flow field:

$$\begin{aligned} U(z) &= 0 \quad \text{for } z \leq 0 \\ &= bz \quad \text{for } 0 \leq z \leq z, \\ &= bz \quad \text{for } z_1 \leq z \end{aligned} \tag{1}$$

Furthermore we assume a time-harmonic plane wave incident from the $z \leq 0$ half space with wave vector $\vec{k}$ and wave number $k = \frac{\omega}{a}$. The entire unperturbed flow field is otherwise assumed to be homogeneous, i.e. no variation for mean densities, temperatures and speeds of sound are allowed.

The velocity potentials ϕ_ℓ and ϕ_u in the lower and upper regions of uniform flow, respectively, bounding the shear layer of thickness z_1 may be taken to be (see for instance Graham and Graham[1] or Miles[7]):*

$$\phi_\ell = \text{R.P.} \left\{ \pm i \left\{ \exp\left[\pm ik(x\sin\theta + z\cos\theta - at) \right] + \right. \right. \\ \left. \left. + \bar{R} \exp\left[\pm ik(x\sin\theta + z\cos\theta - at) \right] \right\} \right\} \quad \text{for } z \leq 0 \tag{2}$$

$$\phi_u = \text{R.P.} \left\{ \pm i\bar{T} \left\{ \exp\left[\pm ik(x\sin\theta \pm (z-z_1)|\sin\theta| \sqrt{\eta_1^2 - 1} - at \right] \right\} \right\} \quad \text{for } z \geq z \tag{3}$$

*The representation of the perturbation fields expressed by equations (2), (3), (4) and (5) is essentially the one used by Graham and Graham[1], although they did neither use the non-dimensional variable η nor the parameter τ (see equations (5) and (8)). At any rate this representation is consistent with the different ones used by Miles and Ribner[8].

In the above equations R.P. denotes "real part of"; the first term in equation (2) represents the incident plane wave of unit amplitude emanating from the half space $z \leq 0$ having wave vector $\vec{k}$ that makes an angle θ with the z-axis as shown in figure 1, with $-\frac{\pi}{2} \leq \theta \leq +\frac{\pi}{2}$; $\bar{R}$ and $\bar{T}$ are the complex reflection and transmission coefficients for the velocity potentials ϕ_ℓ and ϕ_u respectively, i.e.:

$$\begin{aligned} \bar{R} &= R_1 \pm i\, R_2 \\ \bar{T} &= T_1 \pm i\, T_2 \,, \end{aligned} \tag{4}$$

where R_i and T_i are real for the so-called ordinary and amplified reflection regimes and complex in the region of total reflection. In equations (2), (3) and (4) above the upper signs are to be used for $\eta_1 > 1$ (ordinary reflection regime), and the lower signs for $\eta_1 < -1$ (amplified reflection regime); η_1 is the non-dimensional quantity $\eta_1 = \frac{1}{\sin\theta} - M_1$ (see equation (5) below) with $M_1 = \frac{bz_1}{a}$ being the upper fluid Mach number. This choice of signs ensures that the radiation condition, as discussed by Miles[7], Ribner[8] and Graham and Graham[1] is satisfied.

In the shear layer region $0 \leq z \leq z_1$ in which the mean flow varies linearly with z (see equation (1)), it is convenient to use the non-dimensional variable η (see Ref. 5)

$$\eta = \frac{1}{\sin\theta} - \frac{bz}{a} = \frac{1}{\sin\theta} - M(z) \tag{5}$$

where M(z) is the local Mach number of the mean flow in the shear layer. If then one assumes that within the shear layer region the

pressure perturbation $p'(\vec{r},t)$ is of the form:

$$p'(\vec{r},t) = p(z)\sin(k_x x-\omega t) \qquad (6)$$

with $k_x = \vec{k}\cdot\vec{e}_x = \frac{\omega}{a} k \sin\theta$, one obtains the following ordinary differential equation for the z-dependent part p(z) of the pressure perturbation p' in terms of the nondimensional variable η defined by equation (5) (see Koutsoyannis[5]):

$$p_{\eta\eta} - \frac{2}{\eta} p_\eta + (4\tau)^2(\eta^2 - 1)p = 0 \qquad (7)$$

with τ being the parameter defined by:

$$4\tau = \frac{\omega}{b} \sin\theta \qquad (8)$$

We have shown earlier (see Koutsoyannis[5]) that the two independent solutions of equation (7) are:

$$\left.\begin{matrix} f(\eta;\tau) \\ g(\eta;\tau) \end{matrix}\right\} = (4i\tau)^{-\frac{1}{2}\pm m}\, \eta^{\frac{1}{2}} M_{i\tau,\pm m}(4i\tau\eta^2),\ m = \frac{3}{4} \qquad (9)$$

which are real functions of the variable η and the parameter τ for real values of η and τ. Using the above solutions $f(\eta;\tau)$ $g(\eta;\tau)$ one may further write the following general expression for the pressure perturbation $p'(\vec{r},t)$ and the z-component w of the velocity perturbation:

$$p'(\vec{r},t) = p^{(1)}(\eta;\tau)\sin\left[k(x\sin\theta-at)\right] + p^{(2)}(\eta;\tau)\cos\left[k(x\sin\theta-at)\right] \qquad (10)$$

$$w(\eta;\tau) = \frac{a}{4\tau\eta}\left\{ p_\eta^{(1)}(\eta;\tau)\cos\left[k(x\sin\theta - at)\right] - p_\eta^{(2)}(\eta;\tau)\sin\left[k(x\sin\theta - at)\right]\right\} \quad (11)$$

where $p^{(1)}(\eta)$ and $p^{(2)}(\eta)$ are linear combinations of the two independent solutions $f(\eta)$ and $g(\eta)$ (given by equations (9)) of the pressure perturbation equation (7), i.e.

$$p^{(1)}(\eta;\tau) = a_{11}f(\eta;\tau) + a_{12}g(\eta;\tau),\ p^{(2)}(\eta;\tau) = a_{21}f(\eta;\tau) + a_{22}g(\eta;\tau) \quad (12)$$

with a_{ij} constants.

Finally we apply the appropriate boundary conditions at the two edges of the shear layer, at $z = 0$ and $z = z_1$ [or in terms of the non-dimensional variable η (equation (5)) at $\eta_o = \frac{1}{\sin\theta}$ and $\eta_1 = \frac{1}{\sin\theta} - M_1$], namely continuity, of the pressure perturbation p' and of the z-component w of the velocity perturbation.* Then using equations (2), (3), (10), (11) and (12) one may obtain eight linear algebraic equations for the determination of the eight unknowns a_{ij}, R_i and T_i appearing in these equations. After a somewhat tedious

---

*Specifically at $z = 0$ we set:

$$p'(z = 0^-) = -\rho_o \frac{\partial\phi_\ell}{\partial t} = p'(z = 0^+)$$

$$w(z = 0^-) - (\nabla\phi_\ell)\cdot\vec{e}_z = w(z = 0^+)$$

and similarly at $z = z_1$ we set:

$$p'(z = z_1^+) = -\rho_o \frac{D\phi_u}{Dt} = p')z = z_1^-)$$

$$w(z = z_1^+) = (\nabla\phi_u)\cdot\vec{e}_z = w(z = z_1^-)$$

with D/Dt designating the convective name operator in the upper fluid region of constant Mach number M_1.

but straightforward algebra we obtain the following expressions for the square of the reflection coefficient:

$$R^2 = \frac{(A\pm B)^2 + (C\pm D)^2}{(A\mp B)^2 + (C\mp D)^2} \quad , \text{ for } |\eta_1| \geq 1$$

$$|R|^2 = 1 \quad , \text{ for } |\eta_1| \leq 1 \tag{13}$$

where the expressions for A, B, C and D given below involve essentially evaluation of the two independent solutions $f(\eta)$ and $g(\eta)$ of the pressure perturbation given by equations (9) and of their first derivatives at the two edges of the shear layer and are functions of $\eta_o = \frac{1}{\sin\theta}$, $\eta_1 = \frac{1}{\sin\theta} - M_1$ and the parameter τ^* (see equations (5) and (8)).

---

*Using equations (4) for the definitions of the complex reflection and transmission coefficients $\bar{R}$ and $\bar{T}$, respectively, we easily obtain:

$$\begin{aligned} R^2 &= R_1^2 + R_2^2 \\ T^2 &= T_1^2 + T_2^2 \end{aligned} \quad , \text{ for } |\eta_1| \geq 1$$

i.e. in the ordinary and amplified reflection regimes where R_i and T_i are real. In the total reflection regime $|\eta_1| \leq 1$, R_i and T_i are complex and it is also easily obtained that in such as case $|R|^2 = |R_1|^2 + |R_2|^2 = 1$, $\bar{T} = 0$. The meaning of R^2 follows from the interpretation:

$$R^2 = \frac{\text{Reflected Accustic Energy Flux (Time-averaged over one cycle).}}{\text{Incident Acoustic Energy Flux (Time-averaged over one cycle).}}$$

and is discussed in Appendix A.

Explicitly*:

$$A = \frac{1}{4\tau}\left[f_\eta(0)g_\eta(1) - f_\eta(1)g_\eta(0)\right]$$

$$B = 4\tau\sqrt{\eta_o^2 - 1}\sqrt{\eta_1^2 - 1}\left[f(1)g(0) - f(0)g(1)\right]$$

$$C = \sqrt{\eta_1^2 - 1}\left[f(1)g_\eta(0) - f\eta(0)g(1)\right] \qquad (14)$$

$$D = \sqrt{\eta_o^2 - 1}\left[f_\eta(1)g(0) - f(0)g_\eta(1)\right]$$

The upper signs in equations (14) hold for $\eta_1 \geq 1$ and the lower signs for $\eta_1 \leq -1$, in both cases $|\eta_1| \geq 1$, and we have used the notation 0 and 1 in the arguments of f and g and their derivatives with the understanding that 0 designates evaluation at $\eta = \eta_o = \eta\big|_{z=0} = \frac{1}{\sin\theta}$ and 1 designates evaluation at $\eta = \eta_1 = \eta\big|_{z=z_1} = \frac{1}{\sin\theta} - M_1$ i.e., at the two edges of the shear layer. Equation (13) is valid for $-\frac{\pi}{2} \leq \theta \leq +\frac{\pi}{2}$ with the upper signs holding for the regime of ordinary reflection ($\eta_1 > 1$ and $R^2 < 1$) and the lower signs for the regime of the so-called amplified reflection ($\eta_1 \leq -1$, $R^2 \geq 1$). (For the total reflection regime $|R|^2 = 1$, $-1 \leq \eta_1 \leq +1$, $-\frac{\pi}{2} \leq \theta \leq +\frac{\pi}{2}$.) It is seen from equations (13) and (14) that we recover the three reflection regimes:

*For simplicity we have assumed $\sin\theta \geq 0$ in the expressions for A, B, C and D given by equations (14) since for the geometry chosen in Figure 1 resonances and/or Brewster angles for the corresponding vortex sheet cases exist only for $0 \leq \theta \leq \pi/2$. Equations (14) may be made general, i.e. to apply for all values of the incidence angle θ ($-\pi/2 \leq \theta \leq +\pi/2$) by multiplying B and C by $\mathrm{sgn}(\sin\theta)$.

$\eta_1 \geq 1$, $R^2 \leq 1$: Ordinary Reflection Regime

$-1 \leq \eta_1 \leq -1$, $R^2 = 1$: Total Reflection Regime

$\eta_1 \leq -1$, $R^2 \geq 1$: Amplified Reflection Regime

which agree with the results of Graham and Graham[1]. Indeed these regimes are the same as those found by Miles[7] and Ribner[8] for the limiting case of the vortex sheet ($\tau = 0$).

III. Numerical Evaluation of the Energy Reflection Coefficient R^2

We have evaluated numerically the Whittaker M-functions involved in the two independent solutions $f(\eta;\tau)$ and $g(\eta;\tau)$ of the pressure perturbation equation given by equation (9) using the known series representations of f and g as given by Koutsoyannis[5] for relatively small values of η and τ whereas for large values of η and/or τ we have used a numerical technique outlined in Appendix B. Using these values we have then evaluated the functions A, B, C and D given in equation (14) and then the expression for the energy reflection coefficient R^2 given by equation (13). In particular we have chosen ranges of the relevant problem parameters, i.e., angle of incidence θ, upper fluid Mach number M_1 and Strouhal number τ, for which the corresponding vortex sheet (for the same θ and M_1) has one or two resonances and/or one or no Brewster angle.

Figure 2 shows the behavior of the energy reflection coefficient R^2 for the limiting cases of the vortex sheet ($\tau = 0$) and geometrical acoustics ($\tau \to \infty$) for a typical incidence angle $\theta = 30°$, as a function

of the variable $\eta_1 = \frac{1}{\sin\theta} - M_1 = 2 - M_1$, or as a function of the upper fluid Mach number M_1. As is known (see Refs. 7 and 8) the vortex sheet in this case has resonances at $\eta_1 = -\frac{1}{\sin\theta}$ and $\eta_1 = -\frac{1}{\cos\theta}$, i.e. for $M_1 = 4$ and a Brewster angle at $\eta_1 = +\frac{1}{\cos\theta}$, i.e. at $M_1 = 1.134$. In the geometrical acoustics limit ($\tau \to \infty$) the energy reflection coefficient R^2, as a function of η_1, degenerates into the Heaviside-type step function $R^2 = 1 - H(1-\eta_1)$, i.e. $R^2 = 1$ for $\eta_1 < 1$ and $R^2 = 0$ for $\eta_1 > 1$.

Figure 3 shows the variation of the reflection coefficient with upper fluid Mach number M_1 for a number of values of the parameter τ for a fixed angle of incidence of 30°. For 30° angle of incidence the corresponding vortex sheet ($\tau = 0$) has two resonances, i.e., at -1/sin 30° and -1/cos 30° and one Brewster angle at +1/cos 30°. It is seen from the figure that even for very small τ (~0.01) the resonances in the amplified reflection regime disappear and for values of $\tau \geq 0.5$ the amplified reflection regime has degenerated into the total reflection one with $R^2 = 1$. In the ordinary reflection regime in which the corresponding vortex sheet has a Brewster angle at $\eta_1 = +1/\cos(30°)$ it is seen that even for low values of $\tau \sim 0.05$ the Brewster angle has disappeared and there is discernible variation of the reflection coefficient with upper fluid Mach number up to the value $\tau = 1$ that we have calculated.

Figure 4 shows the variation of the reflection coefficient with upper fluid Mach number M_1 for a number of values of the parameter τ and for a fixed angle of incidence of 45°. This is the special case in which the two resonances of the corresponding vortex sheet coalesce and the same holds for the Brewster angles. As in the 30°

angle of incidence case we observe the same behavior in the amplified reflection regime, i.e., fast drop-off from the vortex sheet values with increasing τ and by $\tau \gtrsim 0.5$ the whole amplified reflection regime has coalesced with the total reflection one. In the ordinary reflection regime though we find essentially no variation from the vortex sheet values up to the value $\tau = 1$ calculated. Apparently it takes quite substantial values of $\tau > 1$ for the reflection coefficient to start differing from the values of the corresponding vortex sheet. Finally Figure 5 shows the variation of the reflection coefficient with upper fluid Mach number M_1 with τ as the varying parameter and for a fixed incidence angle θ for which $\sin\theta = 0.8$. The corresponding vortex sheet has only one resonance and no Brewster angle. The general behavior is similar to that observed in Figure 4, i.e., rapid decrease of reflection coefficient values with increasing τ in the amplified reflection regime and imperceptible change from the vortex sheet values in the ordinary reflection regime up to the value $\tau = 1$ calculated.

From the above figures the following general conclusions may be drawn. The finite thickness shear layer shows no resonances and no Brewster angles. Moreover, the values of the reflection coefficient in the amplified reflection regime drop-off substantially from those of the corresponding vortex sheet with increasing τ, even for modest values of τ on the order of ~1, whereas in the ordinary reflection regimes up to $\tau \sim 1$ modest or no significant changes are observed in the reflection coefficient values for the cases in which the corresponding vortex sheet exhibits no Brewster angle. In contrast when the corresponding vortex sheet exhibits a Brewster angle

in the ordinary reflection regime the reflection (and transmission) characteristics of the finite thickness shear layer, as may be surmised from Figure 3, strongly depend on the value of the parameter τ (in addition to the angle of incidence θ and the upper fluid Mach number M_1). This is in contrast to the results of Graham and Graham[1] who for the case of $M_1 = 3$ and $\sin\theta = 0.2$, that they examined as a typical one for the ordinary reflection regime, they have calculated negligible effects due to the finite layer thickness as compared with the corresponding vortex sheet results. The reason is, as may be easily checked, that in their case the corresponding vortex sheet has Brewster angle at $\eta = \frac{1}{\cos\theta} = 1.1021$, i.e. very close to 1 (see Fig. 2) and moreover they have evaluated the variation of R and T as a function of the non-dimensional parameter*:

$$\frac{\text{Shear Layer Thickness}}{\text{Wave Length}} = \frac{\frac{\omega}{a} z_1 \cos}{2\pi} = \frac{\omega}{b} \cdot \frac{bz_1}{a} \cdot \frac{\cos\theta}{2\pi}$$

$$= \frac{\omega}{b} M_1 \frac{\cos\theta}{2\pi}$$

and they considered variations of this parameter from zero to less than 0.2. This range corresponds to variation of our non-dimensional parameter τ from zero to less than 0.02 and since the value $\tau = 0$ characterizes the vortex sheet, it follows that the choice on the

*In actuality the parameter in Ref. 1 is:

$$\frac{\text{Shear Layer Thickness}}{(\text{Incident wave vector component in the z-direction})^{-1}} = \frac{z_1}{(\frac{1}{2\pi} \frac{\omega}{a} \cos\theta)^{-1}} .$$

above parameter in Ref. 1 has been an unfortunate one,* and the range of values of this parameter investigated by Graham and Graham[1] is too close to the vortex sheet value $\tau = 0$.

IV. Limiting Behavior of the Reflection Coefficient

In this section we study analytically the limiting values and forms of the energy reflection coefficient R^2, as given by equation (13), as the parameters τ, θ and M_1 take extreme values by examining the behavior of A, B, C and D in equations (14) for these limiting values. In particular we will be interested in $\tau \to 0$ or $\tau \to \infty$ corresponding to the vortex sheet and geometrical acoustics limits, respectively (see Koutsoyannis[5]), in $\theta \to 0$ or $\theta \to \pm \pi/2$ corresponding to the normal and parallel incidence, respectively, and in $M_1 \to 0$ or $M_1 \to \infty$, i.e., the low and high upper fluid Mach number limits, respectively.

The vortex sheet limit $\tau \to 0$ follows from the known properties of the series solutions $f(\eta)$ and $g(\eta)$ in equation (9) and from equations (14) (see Ref. 5). In this limit $A \to 0$ and $B \to 0$, whereas

$$C \to 3\eta_o^2 \frac{\kappa \operatorname{sgn} \kappa}{\sqrt{1 - \kappa^2}} \sqrt{\eta_1^2 - 1}$$

*Since the parameter used in Ref. 1 does not contain the shear layer profile slope b, one could have anticipated that it is not a suitable non-dimensional parameter that adequately characterizes the scattering characteristics of the shear layer. In contrast our non-dimensional parameter τ as given by equation (8) does characterize the essential features of the problem since it is the product of the Strouhal number ω/b and the sine of the angle of the incident wave vector with the z-axis. (See also Ref. 5 for a detailed discussion on the physical meaning and importance of the parameter τ.)

and

$$D \to -3\eta_1^2 ,$$

and since $\kappa = \sin\theta$, $\eta_1 = \frac{1}{\sin\theta} - M_1$ we obtain from equation (13)

$$R^2 = \left(\frac{C \pm D}{C \mp D}\right)^2 = \left[\frac{(1 - M_1\sin\theta)^2 \pm \sec\theta \sqrt{(1 - M_1\sin\theta)^2 - \sin^2\theta}}{(1 - M_1\sin\theta)^2 \mp \sec\theta \sqrt{(1 - M_1\sin\theta)^2 - \sin^2\theta}}\right]^2 \quad (15)$$

where again M_1 is the upper fluid Mach number and upper signs correspond to ordinary and lower signs to amplified reflection. Equation (15) is the equation for the vortex sheet and agrees with the corresponding results obtained by Miles and Ribner[8].

The limiting form of the reflection coefficient in the limit of (geometrical acoustics) may be obtained using the asymptotic form of the solutions $f(\eta)$ and $g(\eta)$ in equation (9) as $\tau \to \infty$ (see Ref. 5). Instead of using these forms we may argue as follows: Since it has been shown that in the limit $\tau \to \infty$ one recovers both the amplitude and the phase function of geometrical acoustics (see Ref. 5) it follows that the reflection coefficient R^2 in the limit $\tau \to \infty$ has the form consistent with geometrical acoustics, i.e.,

$$\begin{aligned} R^2 &= 0 \quad \text{for} \quad \eta_1 > 1 \\ &= 1 \quad \text{for} \quad \eta_1 < 1 \end{aligned} \quad (16)$$

The limiting form for normal incidence, i.e., $\theta = 0$ is obtained by observing that in this limit

$$\eta_o = \frac{1}{\sin\theta} \to +\infty , \quad \eta_1 = \frac{1}{\sin\theta} - M_1 \to +\infty$$

and also in equations (14)

$$A \to 0 \ , \ B \to 0 \text{ and } C \to -D.$$

Consequently since only ordinary reflection is possible ($\eta_1 > 1$) the reflection coefficient is zero.

The limiting form for parallel incidence $\theta = \pm \pi/2$ i.e., $\sin^2\theta = 1$ is obtained from equations (14) by observing that in this limit

$$A \to \infty \text{ and } C \to \infty$$

and the reflection coefficient

$$R^2 \to \frac{A^2 + C^2}{A^2 + C^2} \to 1$$

The limiting form for $M \to 0$ is obtained again from equations (14) by observing that in this limit

$$A \to 0, \ B \to 0 \text{ and } C \to -D.$$

Consequently again only ordinary reflection is possible ($\eta_1 \to \eta_o = \frac{1}{\sin\theta} > 1$) with the reflection coefficient being zero.

Finally the limiting form of the reflection coefficient for $M \to \infty$ is the same as that for the vortex sheet, equation (15), i.e., $R^2 = 1$ and since as $M \to \infty$ $\eta_1 \to -\infty$ only the amplified reflection regime applies.

We summarize the above limiting forms of the values of the reflection coefficient together with the corresponding regimes (Ordinary, Total or Amplified reflection) in the following table:

	τ		θ		M_1	
	0	∞	0	$\pm \pi/2$	0	∞
Reflection Coefficient R^2	Vortex Sheet Limit Eq. (14)	Geometrical Acoustics Limit	0	1	0	1
Reflection Regime	O., T., A.	O., T., A.	O.	T. A.	O.	A.

In the above table in the bottom line O., T. or A. stand, respectively, for Ordinary, Total or Amplified reflection.

V. Resonances for the Finite Thickness Thin Shear Layer

In this section we present a proof for the nonexistence of resonances for a nonzero but thin shear layer. It is seen from equation (13) for the reflection coefficient R^2 that resonances which may only exist in the amplifying reflection regime ($\eta_1 < -1$) imply that

$$A + B = 0 \quad \text{and} \quad C + D = 0 \tag{17}$$

We found out in deriving equation (15) for the vortex sheet case ($\tau = 0$) that,to the lowest order in τ,$A \to 0$ $B \to 0$ whereas C and D are nonzero and yield the vortex sheet result. We next evaluate A and B to lowest order in τ as follows: We first insert in equations (14) the values for the functions $f(\eta)$ and $g(\eta)$ from equation (9) to the lowest order in τ and then we evaluate A + B at the zeros of C + D and we show that the two equations (17) are incompatible for small but finite τ, the only possibility remaining being that of $\tau = 0$, i.e. the vortex sheet case.

For small τ one may obtain from equation (9) (see Ref. 5):

$$f(\eta;\tau) = 1 - (4\tau)^2\left(\frac{\eta^2}{2} + \frac{\eta^4}{4}\right) + 0(\tau^4)$$
$$g(\eta;\tau) = \eta^3 + (4\tau)^2\left(\frac{\eta^5}{10} - \frac{\eta^7}{14}\right) + 0(\tau^4) \qquad (18)$$

Inserting these values in equation (14) we obtain:

$$A = (4\tau)\left[3(\eta_0 - \eta_1)\eta_0\eta_1(1 - \eta_0\eta_1)\right]$$
$$B = (4\tau)\sqrt{\eta_0^2 - 1}\sqrt{\eta_1^2 - 1}\left(\eta_0^3 - \eta_1^3\right) \qquad (19)$$

Observing that $\eta_o - \eta_1$ is the upper fluid Mach number M_1 we see from equation (19) that the condition A + B = 0 yields:

$$A + B = (4\tau)\left[3\eta_0\eta_1(1 - \eta_0\eta_1) + \sqrt{\eta_0^2 - 1}\sqrt{\eta_1^2 - 1}\left(\eta_0^2 + \eta_1^2 + \eta_0\eta_1\right)\right] = 0 \qquad (20)$$

Equation (20) must be evaluated at the vortex sheet values of η_o, i.e., where C + D = 0, i.e. at the vortex sheet values of η_o and η_1. Using the two known properties of the vortex sheet solution, i.e.

$$\eta_0^2 + \eta_1^2 = \eta_0^2\eta_1^2 \ , \ \eta_0\eta_1 = 1 - \sqrt{M_1^2 + 1}$$

Equation (20) yields:

$$A + B = -(4\tau)(2M_1^3) = 0 \qquad (21)$$

We see that equation (21) is satisfied only if $\tau = 0$ or $M_1 = 0$ or both and consequently the two equations (17) required for the existence of resonances are incompatible to the lowest order in τ;

it follows that the nonzero thickness thin shear layer has no resonances and no Brewster angles.*

One may also prove, in general, on the basis of certain differential properties of the quantities A, B, C and D, equations (14), and the Wronskian of the solutions $f(\eta;\tau)$ and $g(\eta;\tau)$ (equation (9)) of equation (8), that not only the thin shear layer, but also the finite thickness shear layer has no resonances or Brewster angles and more over resonances and Brewster angles are possible if and only if either $\tau = 0$ (the vortex sheet case) or $\tau \to \infty$ (the geometrical acoustics limit (see figure 2).**

VI. Conclusions

We have evaluated numerically the energy reflection coefficient for plane waves incident on a plane shear layer having a linear velocity profile. The numerical computations were based on a

---

*The conditions for the existence of Brewster angles, i.e. $R^2 = 0$, is the same as that for the existence for resonances, i.e. equations (17), except that in this case the ordinary reflection regime ($\eta_1 > 1$) is the relevant one and the proof follows as for the case of the resonances.

**This is true not only for the linear shear layer (equation 1) but also for a finite thickness shear layer of a generally continuous velocity profile. This result and the corresponding studies will be published in a separate following publication concerned with the scattering characteristics of finite thickness shear layers with a continuous velocity profile a special case of which is the shear layer with a linear mean velocity profile of the present study.

representation of the pressure perturbations in the shear layer region in terms of Whittaker M-functions.

We have found that the shear layer exhibits no resonances and no Brewster angles and a separate analytical proof for the nonzero thickness but thin shear layer substantiates the absence of both resonances and Brewster angles for a finite thickness layer. Moreover we have observed that, the behavior of the reflection coefficient depends crucially on the parameter τ, which,as is seen from equation (8),represents a non-dimensional measure of the disturbance Strouhal number with respect to the disturbance Mach number in the mean flow direction. In particular for moderate values of τ the amplified reflection regime degenerates into the total reflection one whereas in the ordinary reflection regime the variation of the reflection coefficient with τ depends on whether the corresponding vortex sheet has a Brewster angle or not. In cases in which the corresponding vortex sheet has a Brewster angle the reflection coefficient is sensitive to changes in τ even for moderate values of τ whereas in the cases in which the corresponding vortex sheet has no Brewster angle the reflection coefficient for moderate values of τ follows rather closely the corresponding vortex sheet values.

The above results indicate that caution should be exercised in modeling planar shear layers by vortex sheets uncritically even in the ordinary reflection regime and even for subsonic relative flows of the two regions bounding the shear layer, a practice customarily followed in current research and applications in noise studies and in aeroacoustics in general (see Ref. 9). Although it is well known

that,the directional characteristics of the reflected and transmitted plane waves scattered by a finite thickness plane parallel shear layer are independent of the details of the velocity profile in the layer (provided that the profile is "smooth") (see for instance Ref. 10), the amplitudes of the transmitted and reflected waves crucially depend on the parameter τ, in addition to the angle of incidence θ and the relative Mach number M of the two uniform flows bounding the finite thickness shear layer. Indeed we have shown that for certain combinations of τ, θ and M, i.e. those for which the corresponding vortex sheet has a Brewster angle (energy reflection coefficient = 0) the scattering characteristics of a finite thickness shear layer may drastically differ from those of the corresponding vortex sheet ($\tau = 0$) even for modest (non-zero) values of τ. Moreover if one allows for different densities and temperatures in the three flow regions ($z \leq 0$, $0 \leq z \leq z_1$ and $z \geq z_1$), a case of particular interest to noise generation by and/or propogation through hot jets, the difference between the scattering characteristics of a finite thickness shear layer and the corresponding vortex sheet characteristics becomes even more pronounced for certain ranges of values and/or combination of the relevent parameters involved. The detailed calculations and the corresponding studies will be published in a following separate publication concerned with the scattering characteristics of a linear shear layer as examined in the present studies but allowing for different densities ρ and speeds of sound in the three regions of mean flow (see Figure 1).

REFERENCES

1. Graham, E.W. & Graham, B.B. Effect of a shear layer on plane waves of sound in fluid. J. Acoust. Soc. Am., 46 (1), 1968, pp. 369-375.
2. Küchemann, D. Störungsbewegungen in einer Gasströmung mit Grenzschicht. Zeit. angew. Math. Mech, 18, 1938, pp. 207-222; see also Görtler, H. ibid, 23, 1943, pp. 1
3. Pridmore-Brown, D.C. Sound propagation in a fluid flowing through an attenuating duct. J.F.M. 4, 1958, pp. 393-406.
4. Goldstein, M. & Rice, E. Effect of shear on duct wall impedance. J. Sound & Vibration, 30 (1), 1973, pp. 79-84.
5. Koutsoyannis, S.P. Features of sound propagation through and stability of a finite shear layer. Advances in Engineering Science, NASA CP-2001, 3, 1976, pp. 851-860; see also 1977 JIAA TR-5, 1978 JIAA TR-12.
6. Jones, D.S. The scattering of sound by a simple shear layer. Phil. Trans., 284A, 1977, pp. 287-328.
7. Scott, J.N. Propagation of sound waves through a linear shear layer, AIAA Journal, 17, 1979, p. 237-244.
8. Miles, J.W. On the reflection of sound at an interface of relative motion. J. Acoust. Soc. Am., 29, 1957, pp 226-228. See also Miles, J.W. On the disturbed motion of a plane vortex sheet. J. Fluid Mech 4, 1958, pp. 538-552.
   Ribner, H.S. Reflection, transmission and amplification of sound by a moving medium. J. Acoust. Soc. Am., 27 (4), 1957, p. 435.
9. Candel, S.M. Application of geometrical techniques to aeroacoustic problems. AIAA paper, 1976, pp. 76-546, Palo Alto, CA.
10. Kornhauser, E.T. Ray theory for moving fluids. J. Acoust. Soc. Am., 25 (5), 1953, pp. 945-951; see also Goldstein, M.E. Aeroacoustics 1974, NASA N74-35118.

11. Blokhintzev, D.I. Acoustics of a nonhomogeneous moving medium. Tekhniko-Theoreticheskoi Literatury, Moskva, 1946, NACA TM 1399.

12. Candel, S.M. Acoustic Conservation principles and an application to plane and model propagation in nozzles and diffusers. J.S.V. 41 (2), 1975, pp. 207-232.

13. Bretherton, F.P. and Garrett, C.J.R. Wavetrains in inhomogeneous moving media, Proc. Roy. Soc. A302, 1969, pp. 529-554.

14. Buchholz, H. Die konfluente hypergeometrische funktion. Springer-Verlag, Berlin-Göttingen-Heidelberg, 1953.

15. Schäfke, F.W. Lösengstypen von difference gleichungen und summengleischungen in normierten abelchen gruppen. Math. Zeitschr. 88, 1965, pp. 61-104.

16. Olver, F.W.J. Numerical solution of second-order linear difference equation. J. Res. Nat. Bur. Standards, Sec. B, 71, 1967, pp. 111-129; see also Olver, F.W.J. and Sookne, D.J. Note on background recurrence algorithms. J. Math. Comput. 26, 1972, 941-947.

APPENDIX A

A.1 Representation of the Velocity Potentials in the Regions $z \leq 0$ and $z \geq z_1$.

(i) Velocity Potential ϕ_ℓ for the Lower Region $z \leq 0$.

Consider an incident plane wave which in coordinates (x,z) fixed in the lower fluid, which is at rest, is a sine wave with wavevector $\vec{k}$ making an angle θ with the z-axis, i.e.

$$\vec{k}.\vec{e}_z = k\cos\theta$$

with $-\frac{\pi}{2} \leq \theta \leq +\frac{\pi}{2}$.

The wave is an upcoming one with amplitude A and thus its potential may be written as:

$$\phi_i = \phi_{incident} = A \sin (k_x x + k_z z - \omega t).$$

And since $k_x = k\sin\theta$, $k_y = k\cos\theta$, $k = \frac{\omega}{a}$

we may further write:

$$\phi_i = A \sin \left[\frac{\omega}{a}(x\sin\theta + z\cos\theta - at)\right]$$

The reflected wave will in general have in phase and out of phase case components; thus since the x-wave number is conserved in this stratified medium we may write for the reflected wave which is a downgoing wave:

$$\phi_r = \phi_{reflected} = A \left[R_1 \sin \frac{\omega}{a}(x\sin\theta - z\cos\theta - at) + R_2 \cos \frac{\omega}{a}(x\sin\theta - z\cos\theta - at)\right]$$

where R_1 and R_2 are respectively the in-phase and out-of-phase components of the reflection coefficient for the velocity potential. Finally

$$\phi_\ell = \text{Total Velocity Potential in the lower region } z \leq 0$$

$$= \phi_i + \phi_r$$

$$= A \left\{ \sin \left[\frac{\omega}{a}(x\sin\theta + z\cos\theta - at) \right] + \right.$$

$$+ R_1 \sin \left[\frac{\omega}{a}(x\sin\theta - z\cos\theta - at) \right] +$$

$$\left. + R_2 \cos \left[\frac{\omega}{a}(x\sin\theta - z\cos\theta - at) \right] \right\}$$

Defining by $\bar{R} = R_1 \pm i\, R_2$, the complex reflection coefficient and taking the amplitude A to be real we may write in complex notation:

$$\phi_e = A \text{ R.P.} \left\{ \pm i \left[e^{\pm i(k_x x + k_z z - \omega t)} + \bar{R} e^{\pm (k_x x - k_z z - \omega t)} \right] \right\}$$

$$= A \text{ R.P.} \left\{ \pm i \left[\cos(k_x x + k_z z - \omega t) \pm i \sin (k_x x + k_z z - \omega t) \right] \right.$$

$$\left. (R_1 \pm iR_2) \left[\cos(k_x x - k_z z - \omega t) \pm i \sin (k_x x - k_z z - \omega t) \right] \right\}$$

$$= A \left\{ \sin(k_x x + k_z z - \omega t) + R_1 \sin (k_x x - k_z z - \omega t) + \right.$$

$$\left. + R_2 \sin (k_x x - k_z z - \omega t) \right\}$$

irrespective of upper or lower signs.

(ii) Velocity Potential ϕ_u in the Upper Region $z \geq z_1$.

The upper medium is moving with uniform velocity

$\vec{U}_1 = bz_1 \vec{e}x$, with $M_1 = \frac{bz_1}{a}$, with respect to the (x,z) - coordinate system which is fixed in the lower fluid (which is at rest).

Since again the x-wave number is conserved in the stratified medium we may write for the velocity potential of the transmitted wave:

$$\phi_u = A \left\{ T_1 \sin \left[k_{Tx}x + k_{Tz}(z-z_1) - \omega t \right] + T_2 \cos \left[k_{Tx}x + k_{Tz}(z-z_1) - \omega t \right] \right\}$$

where T_1 and T_2 are the in-phase and out-of-phase components of the transmitted wave. As before k_{Tx} is obtained from x-wave number conservation, i.e.:

$$k_{Tx} = k_T \sin\beta = k_{ix} = k\sin\theta = \frac{\omega}{a} \sin\theta,$$

where β is the transmitted wave angle, but the z-wave number k_{Tz} of the transmitted wave <u>may only</u> be uniquely <u>specified</u> by applying the radiation condition as postulated by Miles [17]. Namely from geometrical considerations,

$$k_{Tz}^2 = k_T^2 - k_{Tx}^2$$

$$\text{i.e.,} \quad k_{Tz} = \pm \sqrt{k_T^2 - k_{Tx}^2} \quad , \text{ and}$$

k_T is then obtained from conservation of the frequency ω, i.e., since β is the angle that the transmitted wave vector makes with the z-axis, then

$$\omega = ka = k_T c_T = k_T(a + U_1 \sin\beta),$$

which together with the x-wavenumber conservation, and phase speed conservation,

$$\frac{a}{\sin\theta} = \frac{a}{\sin} + U_1 \ ,$$

results in:

$$k_T = k(1-M_1\sin\theta).$$

Finally:

$$k_{Tz} = \pm \sqrt{k^2(1-M_1\sin\theta)^2 - k^2\sin^2\theta}$$

$$= \pm\, k|\sin\theta|\sqrt{\eta_1^2 - 1} \ .$$

Which of the two signs in the expression for k_{Tz} is to be taken, is determined by the radiation conditions as postulated by Miles [7] i.e. + sign for $\eta_1 > 1$, i.e. in the so-called ordinary reflection regime and - sign for $\eta_1 < -1$ i.e. in the so-called amplifying reflection regime.

Finally writing

$$\bar{T} = T_1 \pm i\, T_2$$

and substituting in the expression for ϕ_u we obtain the expression given by eq.(3) in terms of the complex transmisstion coefficient $\bar{T}$.

A.2. Definition of the Energy Reflection Coefficient.

We define the energy reflection coefficient R^2 as

$$R^2 = \frac{\text{Reflected Acoustic Energy Flux Density Averaged Over a Cycle}}{\text{Incident Acoustic Energy Flux Density Averaged over a Cycle}}$$

And since for a plane wave propagating in a medium at rest the energy flux density is $a\rho_0 v'^2$, where v' is the (acoustic) particle velocity in the direction of the plane wave propagation, we may write:

$$v'^2_{\text{incident}} = \left(\frac{\partial \phi_i}{\partial x}\right)^2 + \left(\frac{\partial \phi_i}{\partial z}\right)^2$$

$$v'^2_{\text{reflected}} = \left(\frac{\partial \phi_r}{\partial x}\right)^2 + \left(\frac{\partial \phi_r}{\partial z}\right)^2 ;$$

thus indicating with a bar time averaging over a cycle of the incident monochromatic wave we may further write:

$$R^2 = \frac{\overline{v'^2_{\text{refl.}}}}{\overline{v'^2_{\text{incid.}}}}$$

$$= \frac{A^2 \frac{\omega^2}{a^2} \left\{ R_1^2 \overline{\cos^2 \left[\frac{\omega}{a}(x\sin\theta + z\cos\theta - at)\right]} + R_2^2 \overline{\sin^2 \left[\frac{\omega}{a}(x\sin\theta - z\cos\theta - at)\right]} \right\}}{A^2 \frac{\omega^2}{a^2} \overline{\left[\cos^2 \frac{\omega}{a}(x\sin\ + z\cos\ - at)\right]}}$$

$$= R_1^2 + R_2^2 \quad .$$

A.3 Acoustic Energy Conservation.

Much confusion has resulted in the literature concerning the precise expression and the meaning of acoustic energy conservation in a stratified fluid since the original publication of Blokhintzev's work [11]. The confusion has been compounded by Ribner's [8] analysis as well as by the more recent review by Candel [12]. It is actually a very simple matter to show that in parallel flows what is actually conserved is the time-averaged (0ver one cycle) cross-flow component of the energy flux density in a reference frame moving with the mean local speed, i.e. the conservation principle may be stated as follows:

$$\frac{\overline{p' \vec{v}' \cdot \vec{n}_\perp}}{\omega'/\omega} = \text{const. (independant of z)},$$

where ω' accounts for the usual Doppler factor relating ω (in the (x-z)-frame) and ω' (in the moving frame) and $\vec{n}_\perp$ is the unit normal to the parallel flow direction. The above relation relates and compliments Bretherton and Garret's[13] action principle with the essential difference that whereas the above principle is limited to short wavelengths, our result in the above equation although limited to a statement concerning the time-averaged cross-flow part of the energy density flux of a single monochromatic component, it is valid for all frequencies.

Since the proof of the above statement has not been given anywhere in the literature, we present below a sketch of this proof, with the details to be published elsewhere.

In a medium at rest

$$p' = -\rho_0 \frac{\partial \phi}{\partial t} \text{ and } \vec{v}' = \nabla\phi \text{ , and}$$

$$p'\vec{v}'.\vec{e}_z = -\rho_0 \frac{\partial \phi}{\partial t} \frac{\partial \phi}{\partial z} ;$$

thus for the lower region (which is at rest) we may write, since $\omega = \omega'$,

$$\left(\frac{\overline{p'\vec{v}'.\vec{e}_z}}{\omega'/\omega} \right)_\ell = \frac{-\rho_0}{\omega} \overline{\frac{\partial \phi_\ell}{\partial t} \frac{\partial \phi_\ell}{\partial z}} \quad .$$

$$= \frac{A^2 \rho_0 \omega}{2a} \cos\theta \ (1-R^2) \ .$$

Similarly for the upper region of uniform flow $U_1 = bz_1$, for which

$$p' = -\rho_0 \frac{D_1 \phi_u}{Dt} \ , \quad \vec{v}' = \nabla\phi_u$$

we obtain similarly:

$$\left(\frac{\overline{p'\vec{v}'.\vec{e}_z}}{\omega'/\omega} \right)_u = \frac{-\rho_0}{\omega'} \overline{\frac{D_1 \phi_u}{Dt} \frac{\partial \phi_u}{\partial z}}$$

$$= \frac{A^2 \rho_0 \ k_{Tz} \ T^2}{2} \ \frac{\omega(1-M_1 \sin\theta)}{\omega'}$$

$$= \frac{A^2 \rho_0 \ k_{Tz} \ T^2}{2}$$

Thus energy conservation follows,

$$(1-R^2)\ k_{iz} = T^2\ k_{Tz}$$

where $k_{iz} = k\cos\theta$

and $k_{Tz} = \pm \sqrt{(1-M_1\sin\theta)^2 - \sin^2\theta}$.

APPENDIX B

Numberical Evaluation of the Solutions of $y'' + \left[1 - \frac{2\tau}{x} + \frac{1 - \mu^2}{4x^2}\right] y = 0$

We are concerned with the numberical evaluation of the solutions of the differential equation

$$y'' + \left[\frac{1}{4} - \frac{\tau}{x} + \frac{1 - \mu^2}{4x^2}\right] y = 0 \qquad \text{(B-1)}$$

subject to the coniditon

$$\lim_{x \to o} y(x)/x^{\frac{1+\mu}{2}} = 1 \qquad \text{(B-2)}$$

for arbitrary values of $x > 0$, τ, and $\mu \neq -1, -2, -3, \ldots$

Although power series and asymptotic series exist, they are not really useful for numberical work, especially for "large" values of τ and x. A much better approach is to use the three term recurrence relation and normalization sum for numerical work. This approach allows a numerically stable, unitary, and computationally efficient algorithm which can be used over a very wide range of values of x and τ.

The solutions of equation (B-1) and under dondition (B-2) are

$$S(\tau, + \mu; x) = M_{i\tau, \mu/2}(ix)/(i)^{\frac{1+\mu}{2}}$$

$$S(\tau, - \mu; x) = M_{i\tau, -\mu/2}(ix)/(i)^{\frac{1-\mu}{2}}$$

where $M_{k,m}(z)$ is Whittaker's function.

Using Buchholz [14] we can show that the functions

$$u_j = S(\tau,\mu + 2j;x)\ \frac{\Gamma(\mu + j)}{\Gamma(\mu + 2j)}$$

satisfy the three term recurrence relation

$$\left[\frac{\mu + j - 1}{(\mu + 2j - 1)\ (\mu + 2j - 2)}\right]u_{j+1} - \frac{1}{x} + \left[\frac{2\tau}{(\mu + 2j - 1)\ (\mu + 2j - 2)}\right]u_j +$$

$$\left[\frac{\frac{1}{4}(\mu + 2j + 1)^2 + \tau^2}{(\mu + j)\ (\mu + 2j + 1)\ (\mu + 2j + 2)}\right]u_{j-1} = 0 \qquad \text{(B-4)}$$

and are subject to the normalization relation

$$\sum_{j=0}^{\infty} \lambda_j(\omega)\, u_j = e^{\frac{\omega x}{2}}\ x^{\frac{1+\mu}{2}} \qquad \text{(B-5)}$$

The $\lambda_j(\omega)$ are given by

$$\lambda_j(\omega) = (i)^j\ P_j^{(\frac{\mu-1}{2} + i\tau,\frac{\mu-1}{2} - i\tau)}(-i\omega) \qquad \text{(B-6)}$$

The formulas (B-4), (B-5), (B-6) form the basis of the numerical algorithm. Using the Perron-Kreuser theorem [15], the solutions of (B-4) behave asymptotically as

$$u_{j+1}/u_j \sim + \frac{4}{x}j \quad \text{or } u_j/u_{j+1} \sim \frac{x}{4}\, j^{-1}\ .$$

Using (B-5) and (B-6), we infer that the required solution has the

latter behavior; this solution is called the subdominant solution. The actual numerical algorithm is based upon the algorithm of Olver [16].

Figure 1

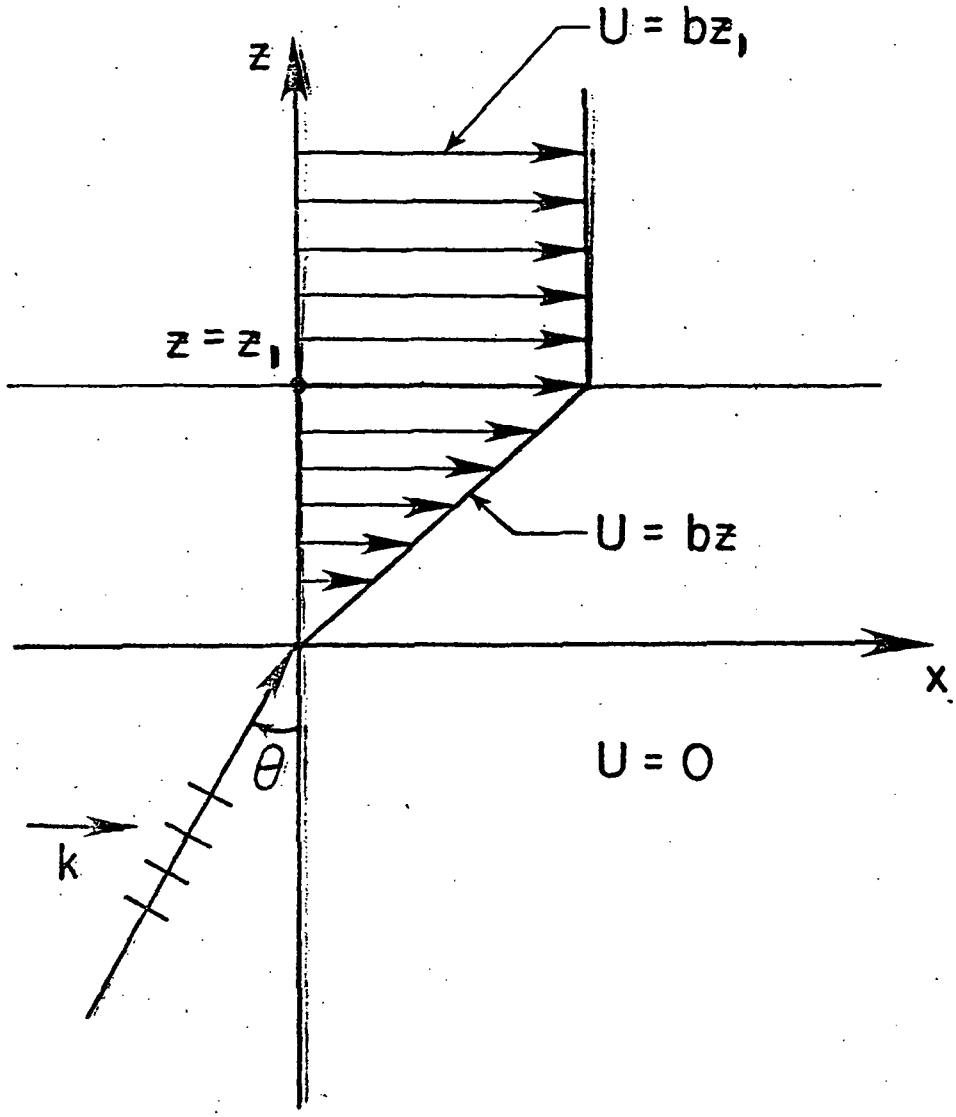

FIGURE 2.

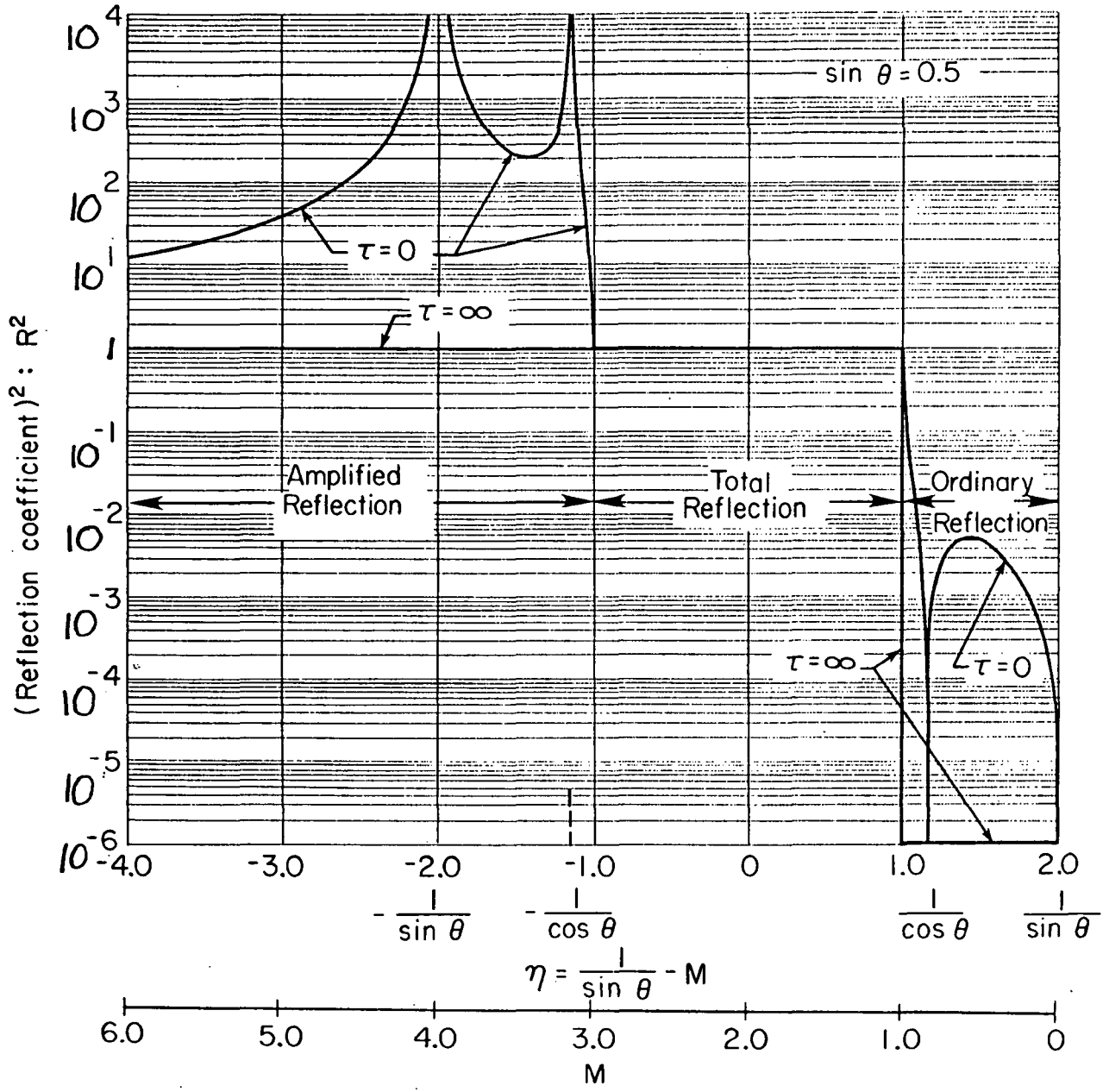
sin θ = 0.5
τ = 0
τ = ∞
Amplified Reflection
Total Reflection
Ordinary Reflection
τ = ∞
τ = 0
(Reflection coefficient)² : R²
10⁴
10³
10²
10¹
1
10⁻¹
10⁻²
10⁻³
10⁻⁴
10⁻⁵
10⁻⁶
-4.0
-3.0
-2.0
-1.0
0
1.0
2.0
-1/sin θ
-1/cos θ
1/cos θ
1/sin θ
η = 1/sin θ - M
6.0
5.0
4.0
3.0
2.0
1.0
0
M

FIGURE 3.

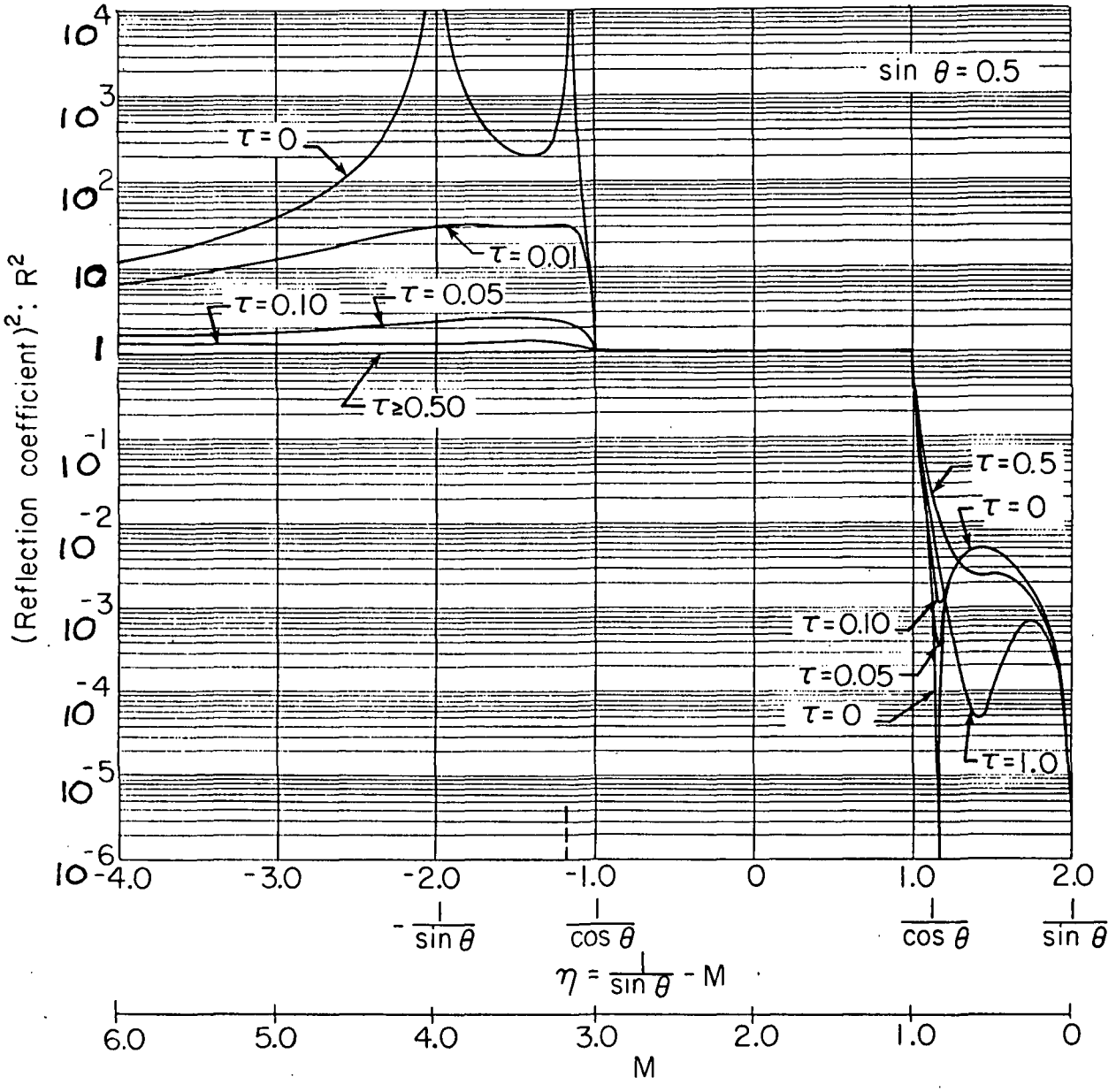
sin θ = 0.5
τ = 0
τ = 0.01
τ = 0.10
τ = 0.05
τ ≥ 0.50
τ = 0.5
τ = 0
τ = 0.10
τ = 0.05
τ = 0
τ = 1.0
(Reflection coefficient)²: R²
10⁴
10³
10²
10
1
10⁻¹
10⁻²
10⁻³
10⁻⁴
10⁻⁵
10⁻⁶
-4.0
-3.0
-2.0
-1.0
0
1.0
2.0
-1/sin θ
1/cos θ
1/cos θ
1/sin θ
η = 1/sin θ - M
6.0
5.0
4.0
3.0
2.0
1.0
0
M

FIGURE 4.

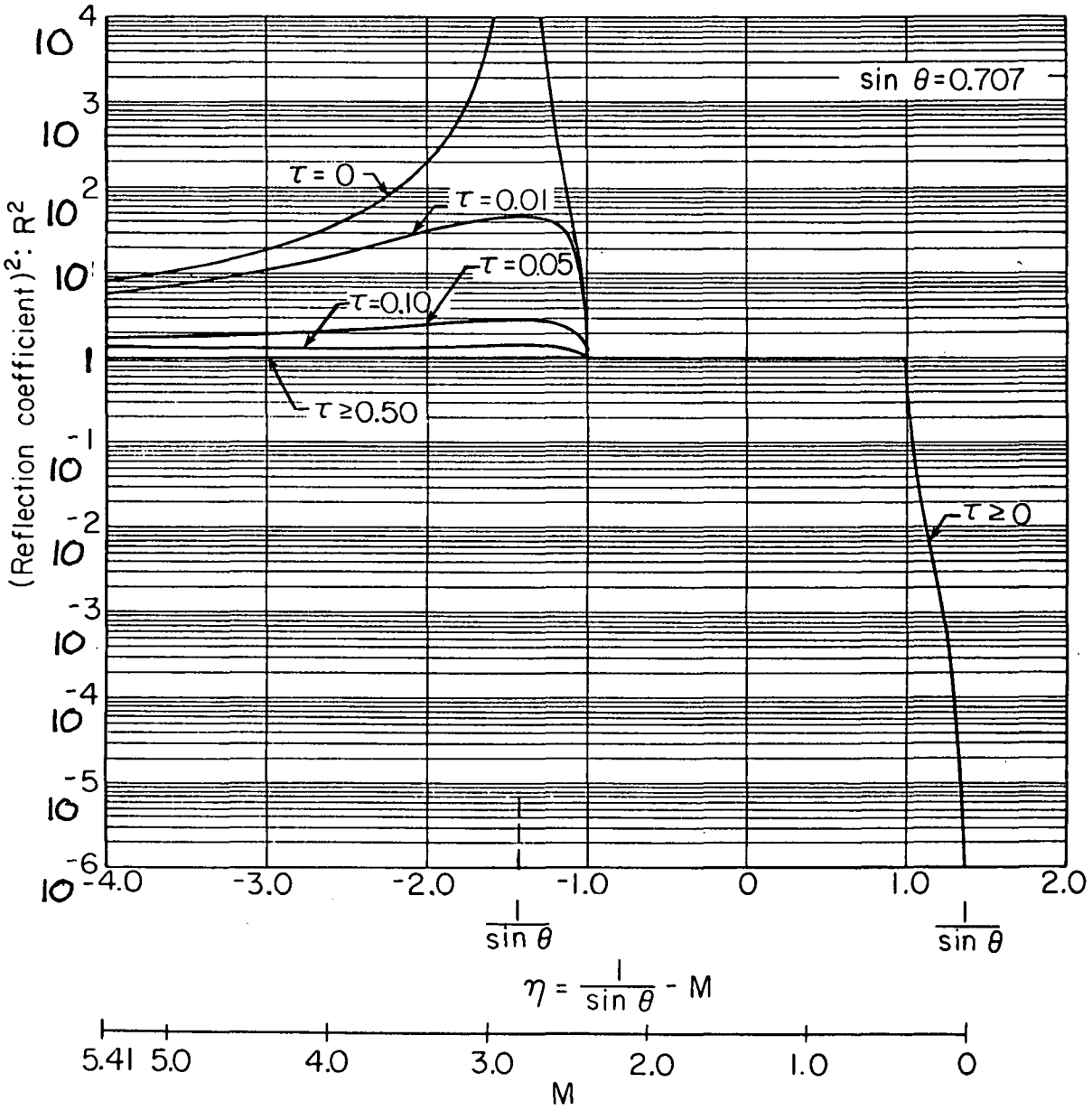
sin θ=0.707
τ = 0
τ = 0.01
τ = 0.05
τ=0.10
τ ≥0.50
τ ≥0
(Reflection coefficient)²: R²
10⁴
10³
10²
10
1
10⁻¹
10⁻²
10⁻³
10⁻⁴
10⁻⁵
10⁻⁶
-4.0
-3.0
-2.0
-1.0
0
1.0
2.0
1/sin θ
1/sin θ
η = 1/sin θ - M
5.41 5.0
4.0
3.0
2.0
1.0
0
M

FIGURE 5.

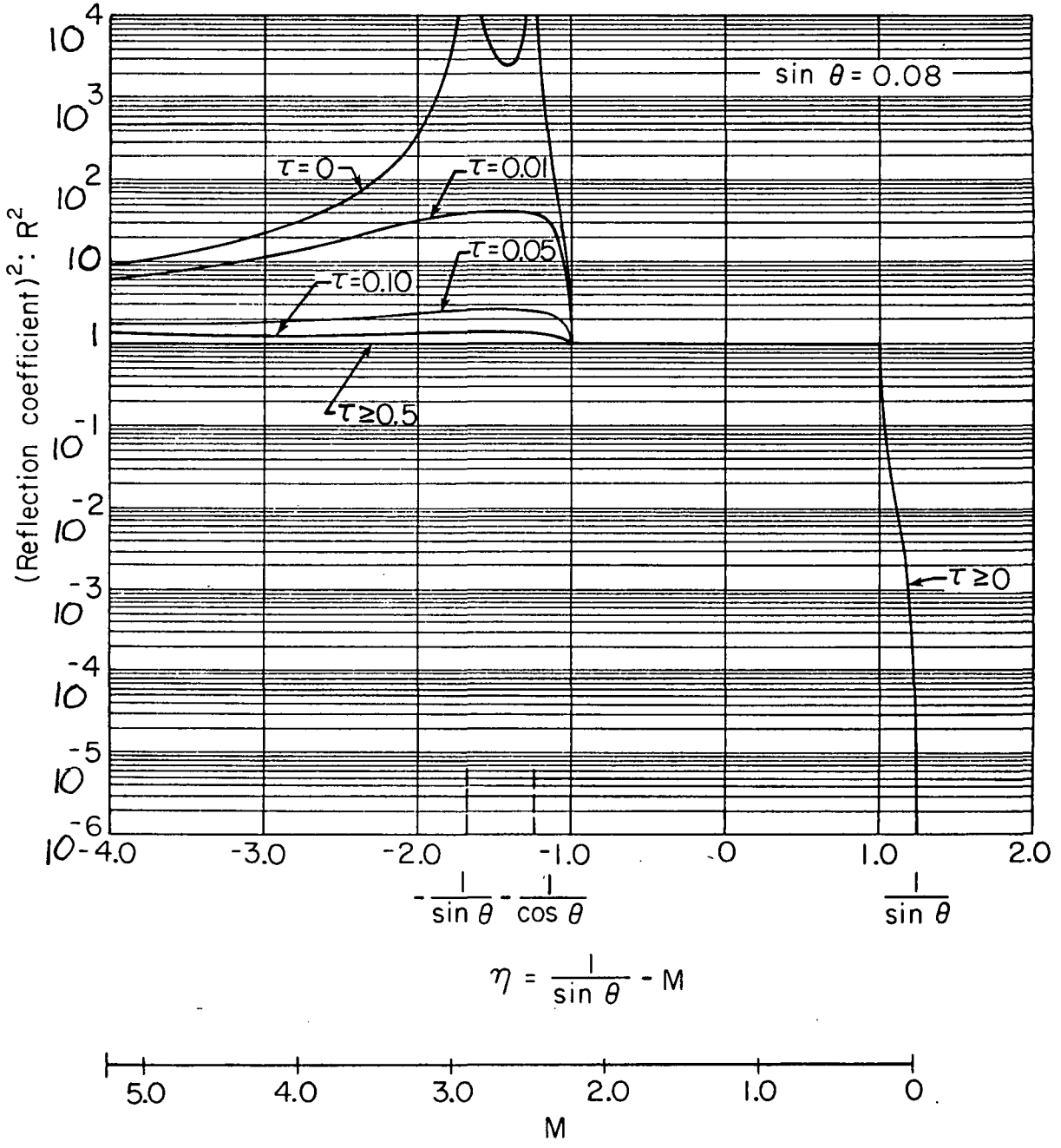
(Reflection coefficient)^2: R^2
10^4
10^3
10^2
10
1
10^{-1}
10^{-2}
10^{-3}
10^{-4}
10^{-5}
10^{-6}
sin θ = 0.08
τ = 0
τ = 0.01
τ = 0.05
τ = 0.10
τ ≥ 0.5
τ ≥ 0
-4.0
-3.0
-2.0
-1.0
0
1.0
2.0
$-\frac{1}{\sin\theta}$
$-\frac{1}{\cos\theta}$
$\frac{1}{\sin\theta}$
$\eta = \frac{1}{\sin\theta} - M$
5.0
4.0
3.0
2.0
1.0
0
M